Sensitivity Maps of Thermodynamic Properties of Carbon Dioxide Near the Critical Point for Optimization in Centrifugal Compressor Design

Pedro Domínguez (Instituto de Ingeniería UNAM)
Oscar De Santiago (ETU i+D S.A. de C.V.)
Héctor Aviña (Instituto de Ingeniería UNAM)

ABSTRACT

The centrifugal compressor is one of the main components within the supercritical carbon dioxide Brayton power cycle, yet the one with the most critical design challenges. This cycle is normally designed so that the compressor operates at inlet conditions close to the critical point of the CO_2 to take advantage of the thermodynamic properties of the fluid. This provides an improvement in cycle efficiency, but implies a challenge in compressor design because slight variations in system conditions lead to significant changes in the physical properties of the fluid. Therefore, it is essential to perform a sensitivity analysis in the vicinity of the critical point to help identify the best behavior path and facilitate decision-making when designing the compressor. This work starts from the equation of state (Span & Wagner) that governs the behavior of carbon dioxide and which is currently reported within the REFPROP database of transport properties and thermodynamics of reference fluids. Through the concept of directional derivative, a thermodynamic sensitivity map is constructed that shows the trajectories of the gradients where the properties of carbon dioxide near the critical point vary more rapidly. The result obtained is a design methodology based on thermodynamic sensitivity maps that facilitates the identification of fluid behavior and can be used to predict compressor performance.

METHODOLOGY

The dimensionless expression of the Helmholtz energy φ is commonly split into a part dependent on the ideal-gas behavior φ^o and a part which takes into account the residual behavior of the fluid φ^r.

$$\varphi(\delta,\tau) = \varphi^o(\delta,\tau) + \varphi^r(\delta,\tau$$

Ideal gas behavior

$$\varphi^o(\delta,\tau) = In(\delta) + {a_1}^o + {a_2}^o\tau + {a_3}^o In(\tau) + \sum_{i=4}^{8} {a_i}^o In\left[1 - e^{(-\tau{\theta_i}^o)}\right]$$

Residual fluid behavior

$$\varphi^r(\delta,\tau) = \sum_{i=1}^{7} n_i \delta^{d_i}\tau^{t_i} + \sum_{i=8}^{34} n_i \delta^{d_i}\tau^{t_i} e^{-\delta^{c_i}} + \sum_{i=35}^{39} n_i \delta^{d_i}\tau^{t_i} e^{-\alpha_i(\delta-\epsilon_i)^2-\beta_i(\tau-\gamma_i)^2} + \sum_{i=40}^{42} n_i \Delta^{b_i}\delta\Psi$$

with

$$\Delta = \theta^2 + B_i[(\delta-1)^2]^{a_i}$$

$$\theta = (1-\tau) + A_i[(\delta-1)^2]^{1/(2\beta_i)}$$

$$\Psi = e^{-C_i(\delta-1)^2 - D_i(\tau-1)^2}$$

The thermodynamic definition for pressure p in relation to the reduced Helmholtz energy φ is

$$p(\delta,\tau) = (1 + \delta{\varphi_\delta}^r)\,\delta\rho_c R\frac{T_c}{\tau}$$

where

$$R = 0.000188924\frac{MJ}{kg\ K}$$

$${\varphi_\delta}^r = \sum_{i=1}^{7} n_i d_i \delta^{d_i-1}\tau^{t_i} + \sum_{i=8}^{34} n_i e^{-\delta^{c_i}}[\delta^{d_i-1}\tau^{t_i}(d_i - c_i\delta^{c_i})] + \sum_{i=35}^{39} n_i \delta^{d_i}\tau^{t_i} e^{-\alpha_i(\delta-\epsilon_i)^2-\beta_i(\tau-\gamma_i)^2}\left[\frac{d_i}{\delta} - 2\alpha_i(\delta-\epsilon_i)\right] + \sum_{i=40}^{42} n_i\left[\Delta^{b_i}\left(\Psi + \delta\frac{\partial\Psi}{\partial\delta}\right) + \frac{\partial\Delta^{b_i}}{\partial\delta}\delta\Psi\right]$$

The directional derivative $D_u f$ enables determining the rate of change of a function of two or more variables in any direction and is defined as:

$$D_u f(x,y) = \nabla f(x,y)\cdot\boldsymbol{u}$$

RESULTS AND DISCUSSION

Fig 1 shows the sensitivity map of the CO_2 pressure p field as a function of reduced inverse temperature τ and reduced density δ. The continuous black lines represent the isobar curves of the field in MPa, the red and blue lines the vapor and liquid saturated curves respectively and the colored arrows the vector field of the rate of change. The CO_2 critical point is located at coordinates $(1,1)$ for $T = T_c$ and $\rho = \rho_c$ .The selected range for this map goes from $200K - 450K$ for temperature and $100\ kg/m^3 - 700\ kg/m^3$ for density focusing on the supercritical zone.

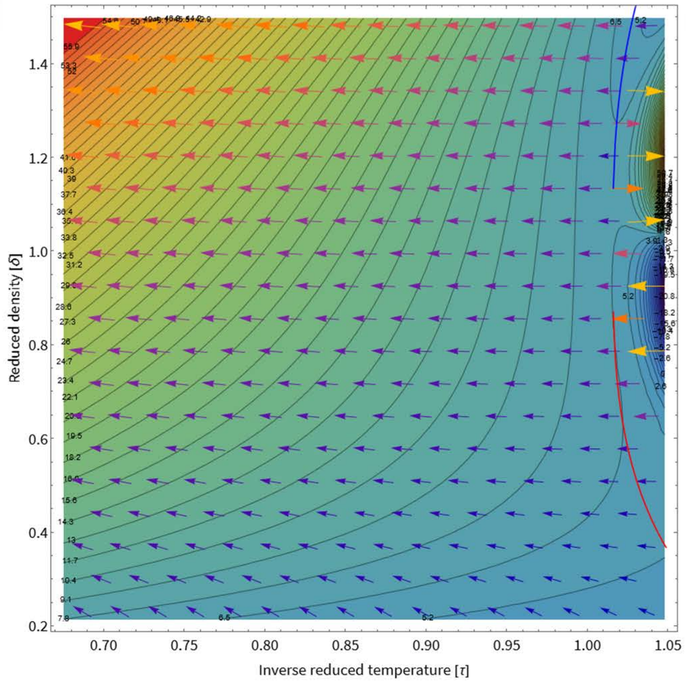

Fig. 1 Pressure gradient in inverse reduced temperature vs reduced density map.

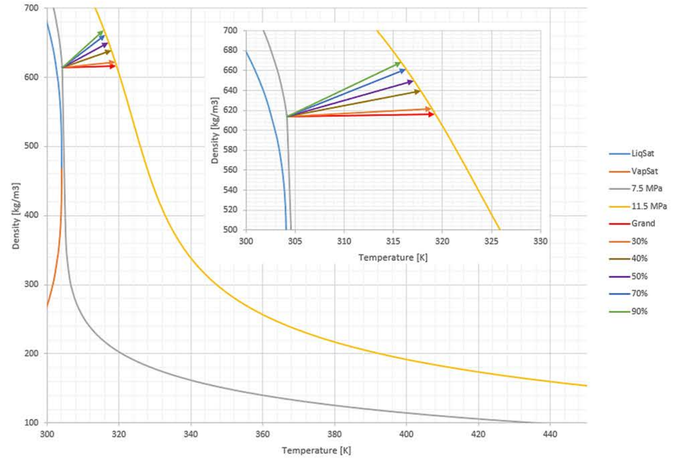

Fig. 2 Compression paths in temperature vs density graph.

Fig. 2 shows the paths of different compression processes starting from a point close to the critical point, where the paths vary as a function of their isentropic efficiency. The rate of change was calculated for five paths from a compressor inlet state defined at 304.15 K and 614.17 kg/m³ starting from a pressure of 7.5 MPa to 11.5 MPa. The gradient vector path is shown as the red arrow. To calculate the value of the gradient for the point defined at the entrance of the compression process, the coordinate $(304.15, 614.17)$ as a function of temperature T and density ρ is passed to its reduced form as a function of δ and τ $(1.313\ , 0.999)$. Applying the gradient to the function $\nabla p(\delta,\tau) = 1.7143, -75.487$ the maximum variation is given by $|\nabla p(\delta,\tau)| = 75.50\ [MPa/s]$.

Table 1. Comparison of paths in the compression process

Efficiency η[%]	Output state (T,ρ)	Paths (δ,τ)	Unit vector (δ,τ)	Rate of change $[MPa/s]$
30	(318,93, 621.53)	(0.0157, -0.0463)	(0.3217, -0.9468)	72.02
40	(317.79, 639.23)	(0.0535, -0.0429)	(0.7805, -0.6250)	48.52
50	(317.08, 649.79)	(0.0761, -0.0408)	(0.8815, -0.4721)	37.15
70	(316.25, 661.78)	(0.1018, -0.0382)	(0.9360, -0.3517)	28.15
90	(315.77, 668.41)	(0.1160, -0.0368)	(0.9531, -0.3024)	24.46

CONCLUSIONS

The rates of change within the compression paths depend on the efficiencies in the process. The lower the efficiency, the more it approximates the direction of the gradient vector. For the example used, the rate of change in paths above 70% efficiency does not increase as much until efficiencies of 90%, below 50% the rate of change increases rapidly. As future work will be implemented in detail the concept of the directional derivative within the design process to identify the best trajectories and areas within the supercritical zone where the variation of the properties does not change too much and can help the understanding of the behavior of supercritical CO_2 in turbomachines

ACKNOWLEDGEMENTS

Thanks to CeMIE-Geo project P08/1125, IIDEA group of the UNAM and ETU i+D S. A. de C. V.

REFERENCES

Brun K., Friedman P. & Dennis R. (2017). Fundamentals and Applications of Supercritical Carbon Dioxide (sCO2) Based Power Cycles. Woodhead Publishing Series in Energy.

Clementoni E. (2021). Comparison of Compressor Performance Map Predictions to Test Daata for a Supecritical Carbon Dioxide Brayton Power System. Proceedings of ASME Turbo Expo 2021 Turbomachinery Technical Conference and Exposition. GT2021-58763. June 7-11, 2021, Virtual, Online.

Span R. & Wagner W. (1996) A New Equation of State for Carbon Dioxide Covering the Fluid Region from the Triple-Point Temperature to 1100 K at Pressures up to 800 MPa, J. Phys. Chem. Ref. Data, 25(6):1509-1596.

Stewart J. (2012), Multivariable Calculus, 7th Edition, Brooks.